

## Characteristics of Surface Roughening during Plane Strain Compression of Polycrystalline Iron

Ichiro Shimizu, Takeji Abe\*, Takayoshi Nosho\*\* and Masahiro Wakayama\*\*\*

The Graduate School of Natural Science and Technology, Okayama University  
3-1-1, Tsushima-Naka, Okayama 700-8530, Japan

\*Department of Mechanical Engineering, Okayama University

\*\*Higashi Okayama Induction Hardening Industries Ltd., Otami, Okayama 703-8228, Japan

\*\*\*Hibi Smelter, Mitsui Mining & Smelting Co. Ltd., Hibi, Tamano, 706-0027, Japan

Roughening behavior of the free surface of polycrystalline iron during plane strain compression is investigated experimentally. The changes in the shape of the free surface, which is roughened during plastic deformation, are observed in the three-dimensions. It is found that the mountains and the valleys of the roughened shape tend to elongate in the constrained direction for the specimen with isotropic grain shape. The shapes of the roughness curves in the loading direction and in the constrained direction are compared. The normalized height distribution of the roughness curve in the constrained direction is symmetric, while that of the roughness curve in the loading direction is asymmetric and positively skew during plane strain compression. Based on a simple simulation of the roughness curves by a random midpoint displacement method, this difference is supposed to be caused by the constraint of the material flow under plane strain condition.

**Key words :** plasticity, surface roughening, plane strain compression, polycrystalline iron, random midpoint displacement method

### 1. INTRODUCTION

Surface roughness appears on the free surfaces of polycrystalline metals during plastic deformation, because polycrystalline metals are microscopically inhomogeneous. The study of the roughening phenomenon is important to investigate the microscopic deformation behavior of polycrystalline metal, and also to clarify the problems related to the surface asperity during precise metal forming processes.

Most of studies on the surface roughening of free surfaces of polycrystalline metals were discussed on the influences of various factors such as grain size [1-3], material property [4, 5] and strain rate [3], on the degree of the roughness evaluated by roughness parameters. The change in the roughness shapes during plastic deformation in terms of the forming limit of metal sheets was discussed in some papers [6, 7]. The characteristics of the roughness shapes during various deformation modes, however, have not been fully investigated.

The aim of this study is to clarify the characteristics of the roughened shape of the free surface during com-

pression test under the plane strain condition, which sometimes occurs during plastic working such as extrusion or forging. The changes in the roughness shape of the free surface of polycrystalline iron during plane strain compression are investigated, and the influence of the macroscopic constraint of material flow on the roughened shape of the free surface is discussed.

### 2. EXPERIMENTAL PROCEDURES

The material used in this experiment is hot-rolled iron with purity of 99.55 wt.%. After specimens are cut into rectangular and parallelepiped shape of  $30 \times 30 \times 20 \text{ mm}^3$ , their free surfaces are finished with abrasive papers and diamond pastes until the centerline average roughness became less than  $0.05 \text{ }\mu\text{m}$ . The specimens are annealed in a vacuum at 1193 K for one hour until the average grain sizes become  $200 \sim 350 \text{ }\mu\text{m}$ . Two kinds of specimens are prepared. One is with the free surface perpendicular to the rolling direction, where the aspect ratio  $R_g$  of the average grain size in the loading direction to that in the transverse direction is  $R_g \cong 1$  on the free surface. The oth-

er is with the free surface parallel to the rolling direction, where  $R_g \cong 1.5$ .

The compression test under the plane strain condition is conducted as shown in Fig. 1. The specimen is compressed in the longitudinal direction, while the parallel sides of the specimen are contacting with the rigid plates. Teflon sheets and carbon grease are used as lubricants between the specimen, plates and the dies, in order to avoid barreling of the specimen.

Three-dimensionally roughened shape of the free surface is measured in the area of about 3 mm square, by a system composed of a stylus instrument and a personal computer [8]. The grain map, which is traced from photos by a scanning electron microscope, is superposed upon the contour map of the roughened shape. Thus, the relation between the roughened shape and deformation of grains is observed.

The roughness profiles of the free surface are measured by a stylus instrument in the loading direction and in the constrained direction, where the measuring length is 12 mm long. The roughness curve  $f(x)$  is obtained by applying the long-wavelength cut-off to the roughness profiles  $F(x)$  as,

$$f(x) = F(x) - \int_{-\infty}^{\infty} S(x) F(t-x) dx \quad (1)$$

$$S(x) = \exp \left( -\frac{\pi x^2}{(\alpha \lambda_c)^2} \right) / \alpha \lambda_c \quad (2)$$

where  $\alpha$  is the constant  $\alpha=0.4697$  and  $\lambda_c$  is the cut-off value [9]. This arithmetic long-wavelength cut-off is the standard method to obtain the roughness curve. Fig. 2 shows the example of an original roughness profile and obtained roughness curve using Eqs. 1 and 2 with cut-off value of 0.8 mm. It must be noticed that the long-wavelength component of the roughness profile is el-

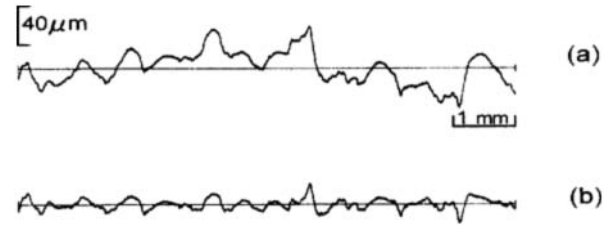


**Fig. 2.** Example of long-wavelength cut-off using Eqs. 1 and 2 with cut-off value of 0.8 mm. (a) Original roughness profile and (b) Roughness curve obtained after cut-off.

minated. The shapes of the mountains and the valleys having wavelengths shorter than the cut-off value, however, are maintained even after the cut-off operation.

The centerline average roughness  $R_a$ , which is the most widely used parameter for surface roughness, is employed in this work and is defined as

$$R_a = \frac{1}{L} \int_0^L |f(x)| dx \quad (3)$$

where  $L$  is the length of the roughness curve.

### 3. EXPERIMENTAL RESULTS AND DISCUSSIONS

Contour maps of the roughened shapes of the specimens having the initial aspect ratio of grains  $R_g=0.94$  and  $R_g=1.49$  on their free surfaces are shown in Figs. 3 and 4, respectively. The thick lines in these figures indicate the grain boundaries. The shapes of the mountains of the roughening shown in Fig. 3(a) are isotropic on the free surface. On the other hand, the shapes of the mountains in Fig. 4(a) are relatively anisotropic, that is, wide in the loading direction. This is because the av-

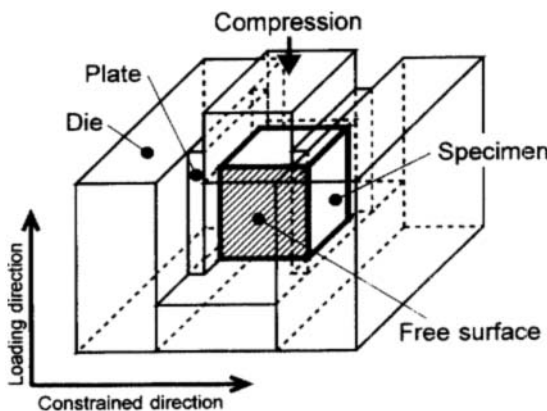


**Fig. 1.** Plane strain compression test.

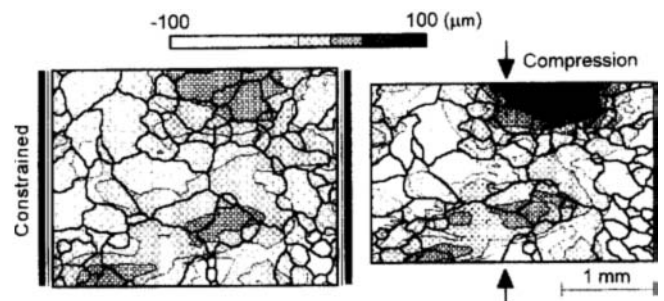


**Fig. 3.** Contour maps of three-dimensional roughened shapes of a free surface. Initial ratio of average grain size in loading direction to that in constrained direction is  $R_g=0.94$ . Thick lines in the figures indicate grain boundaries. (a) Applied strain  $\varepsilon=-0.2$  and (b)  $\varepsilon=-0.4$ .

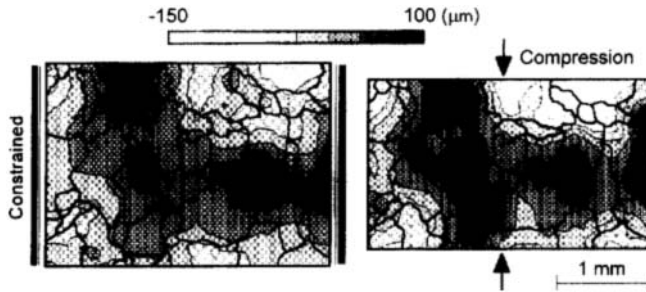


**Fig. 4.** Contour maps of three-dimensional roughened shape of free surface, where  $R_g=1.49$ . (a)  $\varepsilon=-0.2$  and (b)  $\varepsilon=-0.4$ .

average grain size in the loading direction is larger than that in the constrained direction on the free surface shown in Fig. 4 [10]. The mountains become higher in the surface vertical direction and become narrower in the loading direction during plane strain compression (Figs. 3(b) and 4(b)). Their locations for the specific grains, however, scarcely change. This fact means that the roughened shapes shown in Figs. 3 and 4 are mainly formed by the relative rotation of grains [1, 7]. Their changes during plane strain compression are thus corresponding to the deformation of respective grains.

Fig. 5 shows the change in the centerline average roughness  $R_a$  with the equivalent strain. The roughness curves are obtained by the long-wavelength cut-off with the cut-off value of 0.8 mm, which is used to eliminate the influence of barreling of the specimen upon the

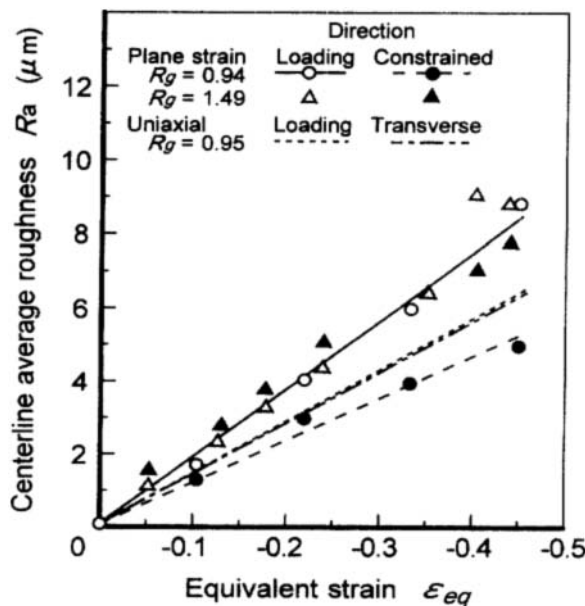


**Fig. 5.** Change in centerline average roughness  $R_a$  with equivalent strain  $\varepsilon_{eq}$ .

roughness parameter. The result of uniaxial compression test of another specimen having the isotropic grain shape ( $R_g=0.95$ ) on its free surface is also shown in Fig. 5. In uniaxial compression, the average roughness in the loading direction is almost the same with that in the transverse direction. On the other hand, the average roughness in the loading direction is larger than that in the constrained direction during plane strain compression, even for the specimen having the isotropic grain shape. This fact is considered as one of the important characteristics of the roughening of the free surface under plane strain compression. For the specimen having the anisotropic grain shape ( $R_g \cong 1.5$ ), however, the average roughness in the loading direction is about the same with that in the constrained direction during plane strain compression.

Examples of the roughness curves in the loading direction and in the constrained direction are shown in Figs. 6(a) and (b), respectively, for the applied strain  $\varepsilon=-0.4$ . The roughness curve in the loading direction seems to have several sharp and deep valleys, compared with that in the constrained direction. In order to characterize the difference between these roughness curves quantitatively, the height distribution is introduced [11]. The height distribution of a roughness curve  $f(h)$  is constructed by taking height  $h$  as an abscissa and fractional area  $S(h)$  as its ordinate. The fractional area for an arbitrary height  $h_i$  is

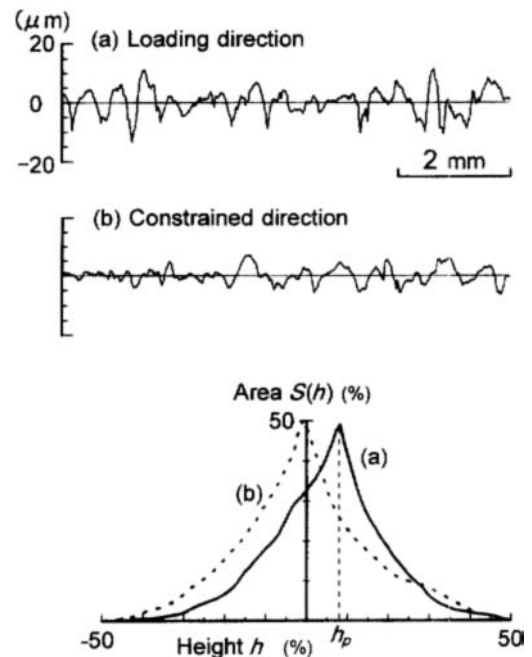


**Fig. 6.** Examples of roughness curves and their normalized height distributions at applied strain  $\varepsilon=-0.4$ .

obtained as

$$S(h_i) = \begin{cases} \int_{h_i}^{h_{max}} |f(h)| dh & (h_i \geq h_c) \\ \int_{h_{min}}^{h_i} |f(h)| dh & (h_i < h_c) \end{cases} \quad (4)$$

where  $h_{max}$  and  $h_{min}$  are the maximum and the minimum height of the roughness curve, and  $h_c$  is the height of the centerline. The normalized height distribution obtained for each curve is also shown in Fig. 6. The roughness curve in the constrained direction has a symmetrical height distribution, while that in the loading direction has an asymmetrical and positively skew one. The degree of the skewness of the height distribution can be represented by the coordinate of the peak of the height distribution  $h_p$ . Fig. 7 shows the averaged skewness  $\bar{h}_p$  of the roughness curves in respective directions. The skewness  $\bar{h}_p$  of the roughness curve in the loading direction increases with the applied strain and becomes about ten percent at  $\varepsilon = -0.4$ , while that of the roughness curves in the constrained direction scarcely changes. This result means that the sharp and deep valleys of the roughened shape are formed only in the direction parallel to the constrained direction. It is considered that the formation of such valley is caused by the constraint of the macroscopic material flow during plane strain compression, that is, the material preferentially flow in the loading

direction and in the perpendicular direction to the free surface.

In order to confirm the influences of the preferential direction of the material flow on the roughening phenomenon, a simple simulation is performed by using a random midpoint displacement method [12]. The formation of a roughness profile by this method shown in Fig. 8 is performed by the following steps: 1) Set a straight line with length of 8 mm (Fig. 8(a)). 2) Offset the midpoint of the line by some Gaussian random  $\Delta h$  with mean  $m$  and standard deviation  $\sigma_1 = 100 \mu\text{m}$ , which is roughly corresponding to the  $R_a$  of a roughness profile at  $\varepsilon = -0.4$  (Fig. 8(b)). 3) Repeat the offset operation on the midpoints of respective segments of the line by Gaussian random with mean  $m$  and standard deviation  $\sigma_n = 2^{-(n+1)/2} \cdot \sigma_1$  at  $n$ -th operation (Fig. 8(d)). The maximum of the repeat number  $n_{max}$  is set as  $n_{max} = 12$  in this simulation, thus the final profile are composed of 4096 segments. The successive midpoint displacements are corresponding to the formation of roughness profile components having different wavelengths. The roughness curve is obtained by applying the long-wavelength cut-off with the cut-off value of 0.8 mm to the composed roughness profile. The simulated roughness curves and their height distribution with  $m=0$ ,  $0.5\sigma_n$  and  $\sigma_n$  of the Gaussian random distribution are shown in Fig. 9 (a), (b) and (c), respectively. The positive offset of the Gaussian distribution corresponds to strengthen the material flow in the perpendicular direction to the free surface. It is

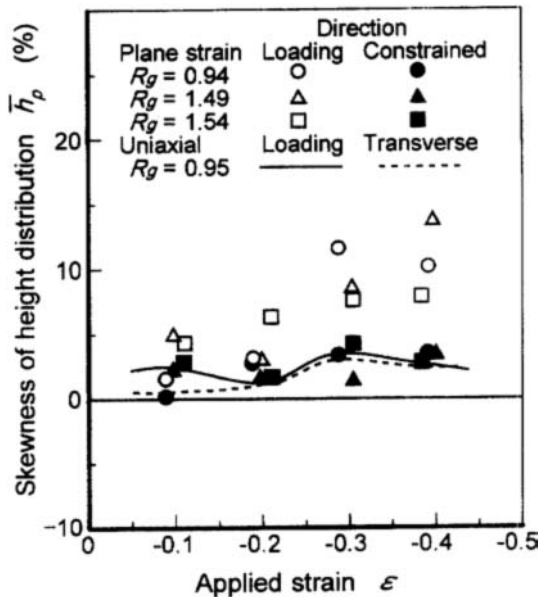


Fig. 7. Change in averaged skewness  $\bar{h}_p$  of roughness curves in loading direction and in constrained direction with applied strain.

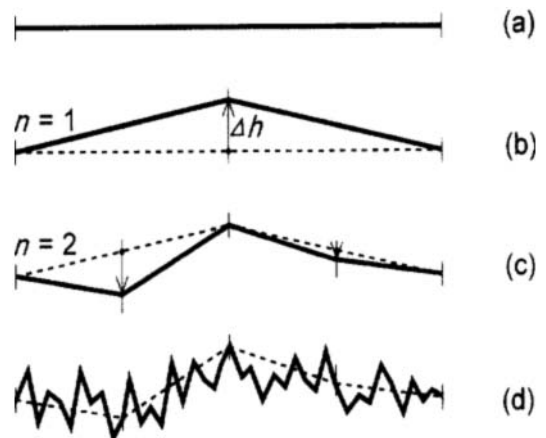
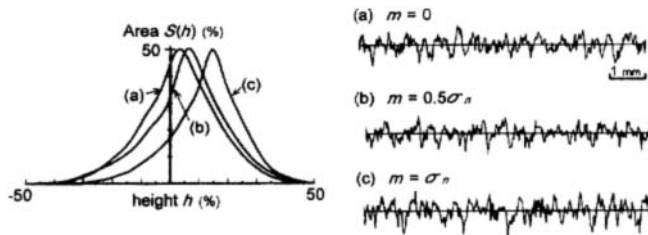


Fig. 8. Construction of a roughness profile by a random midpoint displacement method. The displacement  $\Delta h$  is decided by a Gaussian random distribution. (a) Initial straight line, (b) Profile after the first midpoint displacement operation, (c) Profile after the second operation and (d) Profile after the  $n$ -th operation.



**Fig. 9.** Simulations of roughness curves and their height distribution by means of random midpoint displacement method, where  $m$  is offset parameter and  $\sigma_n$  is standard deviation of Gaussian random distribution at  $n$ -th operation.

seen that the simulated roughness curve with  $m=0$  shows the symmetrical height distribution. On the other hand, several deep and sharp valleys appear on the roughness curves with  $m=0.5\sigma_n$  and  $\sigma_n$ , their height distribution profiles thus become asymmetrical and positively skew. These facts suggest that the height distribution of the roughness curve be skew due to the preferential material flow in the perpendicular direction to the free surface.

Based on the results discussed above, the formation mechanism of the roughness curve during plane strain compression is considered as follows. At the early stage of plastic deformation, the roughness curve is mainly formed by relative rotations among grains and has symmetrical height distribution. With the following compressive deformation under plane strain condition, several deep and sharp valleys appear on the roughness curve in the loading direction due to the preferential material flow in the perpendicular direction to the free surface. Besides, the compressive deformation in the loading direction makes the valleys sharper. The height distribution of the roughness curve is thus positively skew with the applied strain.

#### 4. CONCLUSION

1. Surface roughening of free surface of polycrystalline iron is mainly formed by relative rotations among grains during plane strain compression. The change in the roughened shape during compression cor-

responds to the deformation of respective grains.

2. The average roughness measured in the loading direction becomes larger than that in the constrained direction on the free surface having isotropic grain shape. The roughness degrees in both directions, however, are almost the same when the average grain size in the loading direction is about 1.5 times larger than that in the constrained direction.

3. The height distribution of the roughness curve in the loading direction is positively skew with the applied strain. This is because several sharp and deep valleys appear on the free surface, due to the preferential material flow in the perpendicular direction to the free surface. This characteristic is also seen in the simulation of roughness curve by the random midpoint displacement method, with positive offset of Gaussian random distribution.

#### REFERENCES

1. K. Osakada and M. Oyane, *Bull. JSME* **14-68**, 171 (1971).
2. C. Guangnan, S. Huan, H. Shiguang and B. Baudalet, *Mater. Sci. Eng.* **A128**, 33 (1990).
3. A. Azushima and M. Miyagawa, *J. of the Jpn. Soc. for Tech. of Plasticity* **27-310**, 423 (1986).
4. P. F. Thomson and P. U. Nayak, *Int. J. of Mach. Tool Des. Res.* **20**, 73 (1980).
5. P. F. Thomson and P. U. Nayak, *Int. J. of Mach. Tool Des. Res.* **22**, 261 (1982).
6. K. Yamaguchi, N. Takakura and M. Fukuda, *Computational Plasticity* (eds., T. Inoue, H. Kitagawa and S. Shima), p. 179, Elsevier Applied Science (1990).
7. Y. Z. Dai and F. P. Chiang, *Trans. ASME, J. of Eng. Mat. Tech.* **144**, 423 (1992).
8. I. Shimizu and T. Abe, *JSME Int. J.* **37A**, 403 (1994).
9. *Tokyo Seimitsu Technical Bulletin*, 9-25, 18 (1992).
10. T. Abe, I. Shimizu and T. Nishiyama, *JSME Int. J.* **35**, 462 (1992).
11. R. S. Sayles, in *Rough Surfaces* (ed., T. R. Thomas), p. 99, Longman, NY (1982).
12. M. F. Barnsley, R. L. Devaney, B. B. Mandelbrot, H. - O. Peitgen, D. Saupe and R. F. Voss, *The Science of Fractal Images*, p. 74, Springer-Verlag (1988).